J. Chem. Thermodynamics 194 (2024) 107287

Contents lists available at ScienceDirect

The Journal of Chemical Thermodynamics

journal homepage: www.journals.elsevier.com/the-journal-of-chemical-thermodynamics

Measurement and modelling of liquid density (298.15 and 313.15 K) and vapour pressure osmometry (313.15 K) for binary aqueous solutions of organic salts

Pedro Velho [a,b,*], Eduardo Sousa [a,b], Eugenia A. Macedo [a,b,*]

[a] LSRE-LCM – Laboratory of Separation and Reaction Engineering - Laboratory of Catalysis and Materials, Faculty of Engineering, University of Porto, Rua Dr. Roberto Frias, 4200-465 Porto, Portugal
[b] ALiCE – Associate Laboratory in Chemical Engineering, Faculty of Engineering, University of Porto, Rua Dr. Roberto Frias, 4200-465 Porto, Portugal

ARTICLE INFO

Keywords:
Electrolytes
Organic salts
Vapour pressure osmometry
Osmotic coefficients
Activity coefficients
Extended Pitzer Model of Archer

ABSTRACT

Due to the eco-friendliness of organic salts, they have been gradually replacing other electrolytes in different fields of chemistry. For example, they provide biocompatible salting-out agents for liquid–liquid extractions and earth-abundant materials for flow batteries. Nevertheless, reliable liquid density and vapour pressure data, which are paramount for a proper parameterisation of thermodynamic models, are often hard to find for aqueous solutions of organic salts, delaying the development of these technologies.

In this work, the liquid density (ρ) of five binary aqueous solutions of organic salts (disodium tartrate, sodium potassium tartrate, dipotassium tartrate, trisodium citrate and tripotassium citrate) were measured and correlated at 298.15 and 313.15 K and 0.1 MPa. In these assays, second-degree polynomials provided determination coefficients (R^2) larger than 0.9982 in the correlation of liquid density with salt molality, for which a very accurate description of this property was accomplished. Moreover, vapour pressure osmometry (VPO) studies were carried out for these solutions at 313.15 K and 0.1 MPa. Then, the obtained osmotic coefficients (ϕ) were successfully modelled using the Extended Pitzer Model of Archer, yielding standard deviations (σ_ϕ) lower than $8.61 \cdot 10^{-3}$. Finally, the mean molal activity coefficients ($\gamma_\pm$) and excess Gibbs free energies (G^E/RT) of the binary aqueous solutions of organic salts were effectively calculated, with potassium- and tartrate-based salts attaining significantly higher values than the ones composed of sodium and citrate, hinting at a more ideal solution behaviour of the former.

1. Introduction

The success of a greener approach to chemical manufacturing relies on the measured substitution of classical production routes by eco-friendlier alternatives, aiming at boosting atom economy and reducing waste generation. These objectives constitute two of the twelve principles of Green Chemistry [1], which have been shaping this branch of science over the last decades.

However, the optimization of chemical processes involving electrolytes is more intricate than others due to remarkably complex and unpredictable behaviour, for which this area of chemistry has evolved at slower pace towards enhanced sustainability. Even though electrolytes play an important role in a plethora of processes (*e.g.*, wastewater treatment, seawater desalination and extractive distillation [2,3]), their presence in solution is known to advocate non-ideal behaviour, which hardens the description of these systems using classical thermodynamics. For that reason, reliable vapour pressure (p) and liquid density (ρ) data are essential for the improvement and accurate parameterisation of excess Gibbs free energy models and equations of state [4–6].

Most thermodynamic models for electrolyte-containing solutions include specific terms to describe electrostatic interactions [7], which are either based on the Debye-Hückel (DH) [8] or mean spherical approximation (MSA) [9,10] theories. The derivation of the Debye–Hückel theory [8] considers a “cloud” of counterions surrounding each ion and is still widely applied for dilute solutions of 1:1 electrolytes up to 0.01 mol/L. Yet, its application should not be limited to this concentration range since the validity of the theoretical considerations strongly depends on model derivation, solvent properties and

* Corresponding authors.
E-mail addresses: velho@fe.up.pt (P. Velho), eamacedo@fe.up.pt (E.A. Macedo).

https://doi.org/10.1016/j.jct.2024.107287
Received 3 January 2024; Received in revised form 12 March 2024; Accepted 13 March 2024
Available online 15 March 2024

temperature [3].

The Pitzer equations [11], which are the most applied for aqueous solutions of strong electrolytes, include an empirical modification of the Debye-Hückel term expressing the DH limiting law, and provide valuable tools for the determination of a comprehensive suite of thermodynamic properties over a wide range of temperatures and pressures [12]. The Pitzer model quantifies particle interactions by linear combinations of parameters obtained from a virial expansion of the excess Gibbs free energy [13]. Similarly to the Debye-Hückel postulates, this model requires a considerable number of parameters [14], and is expected to better describe symmetrical electrolytes [3], *i.e.*, electrolytes in which the cation and anion have similar dimensions and properties. Moreover, the Pitzer equations were originally formulated for aqueous solutions of electrolytes up to 6 mol/L and their parameters can be estimated based on, for example, osmotic coefficients, activity coefficients and solubility data [12,15].

The description of osmotic (ϕ) and activity (γ) coefficients by the Pitzer equations was later improved by Archer [16,17], which included a dependence of the third virial coefficient with ionic strength by adding an extra adjustable parameter [18]. This extension of the original Pitzer model has proved application on binary vapour-liquid equilibria (VLE) involving molten [6,19,20] and metallic inorganic [21–23] salts, but there is a significant lack of data on systems composed of organic salts.

Given their high biodegradability, organic salts have been extensively applied in the development of green Aqueous Two-Phase Systems (ATPS), which are considered promising liquid–liquid extractive methodologies for biomolecules (*e.g.*, antioxidants [24–26] and proteins [27,28]) and pharmaceutical pollutants (*e.g.*, antibiotics [29] and antimicrobials [29,30]). Moreover, organic salts are expected to play a very important role in the partial replacement of rare metals with more earth-available components in batteries, contributing to more thermodynamically stable and cost-effective assemblies [31,32]. Thus, for the advancement of these technologies, more precise thermodynamic models are needed, which in turn require abundant experimental data on liquid density and vapour pressure.

In this work, the liquid density of five binary aqueous solutions of organic salts (disodium tartrate, sodium potassium tartrate, dipotassium tartrate, trisodium citrate and tripotassium citrate) were measured and correlated at 298.15 and 313.15 K and 0.1 MPa. Furthermore, vapour pressure osmometry (VPO) studies were performed for these solutions at 313.15 K and 0.1 MPa, and the Extended Pitzer Model of Archer was applied in the thermodynamic modelling of osmotic coefficients.

2. Procedure

2.1. Materials

The list of chemical components used in this work and of their respective suppliers, purities, Chemical Abstracts Service (CAS) numbers and abbreviations are shown in Table 1. Moreover, no additional purification steps were performed since the chemicals were recently acquired. The chemical structures of the organic salts can be found in Fig. S1, in the Supplementary Materials.

2.2. Equipment

In this work, mass (m) was determined using an Adam Equipment AAA 250L balance, with standard measurement uncertainty of 10^{-4} g, while liquid density (ρ) was measured at 298.15 and 313.15 K and 0.1 MPa using an Anton Paar DSA-4500 M oscillating U-tube densimeter, with standard measurement uncertainties of $3{\cdot}10^{-5}$ g·cm^{3} and 0.1 K. Moreover, vapour pressure osmometry studies were performed at 313.15 K and 0.1 MPa using a Knauer K-7000 vapour pressure osmometer (VPO), with relative measurement uncertainty of 0.01 and standard measurement uncertainty of 0.1 K in cell temperature. Finally, a Mettler Toledo C20 Coulometric Karl Fisher titrator, with standard measurement uncertainty of 5 ppm, was used to estimate water content, and electrical conductivities (κ) were determined with a Hanna EDGE EC conductivity meter, coupled with a platinum conductivity cell HI763100, with relative measurement uncertainty of 0.01.

Table 1
List of chemical components, with respective chemical formula, supplier, purity, CAS number and abbreviation.

Chemical	Supplier	Purity / % [a]	CAS	Abbreviation [b]
Dipotassium L-tartrate hemihydrate ($C_4H_4K_2O_6{\cdot}0.5H_2O$)	Thermo Scientific	> 99.9	6100-19-2	K_2Tartrate
Disodium tartrate dihydrate ($C_4H_4Na_2O_6{\cdot}2H_2O$)	VWR chemicals	> 99.9	6106-24-7	Na_2Tartrate
Ethanol (C_2H_6O)	Sigma-Aldrich	> 99.0	64-17-5	EtOH
HiPerSolv CHROMANORM water (H_2O)	VWR Chemicals	[c]	7732-18-5	W
Sodium chloride (NaCl)	Merck	> 99.5	7647-14-5	–
Sodium potassium tartrate tetrahydrate ($C_4H_4NaKO_6{\cdot}4H_2O$)	Sigma-Aldrich	> 99.0	6381-59-5	NaKTartrate
Tripotassium citrate monohydrate ($C_6H_5K_3O_7{\cdot}H_2O$)	Sigma-Aldrich	> 99.0	6100-05-6	K_3Citrate
Trisodium citrate dihydrate ($C_6H_5Na_3O_7{\cdot}2H_2O$)	VWR chemicals	> 99.0	6132-04-3	Na_3Citrate

[a] Provided by the supplier in mass percentage. No additional purification steps were conducted.
[b] In the organic salts, abbreviations refer to anhydrous moieties.
[c] The electrical conductivity (κ) of pure water was found to be $5{\cdot}10^{-6}$ S·m^{-1}.

2.3. Sample preparation

For each binary system, 15 different solutions were prepared, covering all the concentration range measurable by the vapour pressure osmometer (VPO) and limited by the solubility of the studied salts at 298.15 K and 0.1 MPa. To do so, pure water (HiPerSolv CHROMANORM water, $\kappa = 5{\cdot}10^{-6}$ S·m^{-1}) and aqueous solutions of the organic salts (Na_2Tartrate: 23.0 % in mass; NaKTartrate: 38.9 % in mass; K_2Tartrate: 19.1 % in mass; Na_3Citrate: 32.6 % in mass; K_3Citrate: 38.8 % in mass) were pipetted and weighed into 15 mL vials. Prior to solubilisation, the water content of the organic salts was confirmed to be the one provided by the commercial suppliers using a Mettler Toledo C20 Coulometric Karl Fisher titrator, with standard measurement uncertainty of 5 ppm. Moreover, during solution preparation, hydrate water was accounted for in the calculation of final molalities.

2.4. Density measurement and correlation

The liquid density (ρ) of the prepared solutions was assessed at 298.15 and 313.15 K and 0.1 MPa using the Anton Paar DSA-4500 M oscillating U-tube densimeter. After having calibrated the equipment with water according to the technical manual, needleless syringes were used to introduce the samples of approximately 1.5 mL in the densimeter. Then, the obtained density of water was validated with data from literature [33], as Fig. S2 and Table S1, in the Supplementary Materials, show. Finally, density measurements of the prepared solutions were performed in triplicate and the cell was cleaned with pure water and ethanol between determinations. The density data were fitted to second-degree polynomials, as equation (1) shows.

$$\rho = \rho_0 + \rho_1 \cdot m + \rho_2 \cdot m^2 \quad (1)$$

where ρ is liquid density (in kg·m^{-3}), m is molality (mol·kg^{-1}) and ρ_0, ρ_1

and ρ_2 are adjustable parameters.

2.5. VPO measurement and modelling

In the vapour pressure osmometry (VPO) studies at 0.1 MPa, a Knauer K-7000 vapour pressure osmometer was used, in which two thermistors are positioned side-by-side in a glass cell saturated with solvent (water) vapour. The VPO measurements were only performed at 313.15 K, following a recommendation present in the osmometer user manual which advises for a difference of 5 to 10 K between room and assay temperatures for more reliable and stable measurements. First, a reference baseline was established by placing a droplet of pure water in each of the thermistors (thermistors 1 and 2) using microsyringes. After letting the osmometer stabilise for 2 h, reading was adjusted to zero. Then, one droplet was kept as pure solvent (thermistor 1) while the other (thermistor 2) was sequentially replaced by droplets of the prepared solutions with growing concentration, as Fig. 1 shows. Five measurements were performed for each solution and each sample droplet was left settling for 10 min. Moreover, thermistor 2 was thoroughly cleaned with pure water between measurements, and similar droplets (size-wise and shape-wise) were maintained in both thermistors to ensure an accurate measurement. As it is well known, the presence of electrolytes causes a decrease in the vapour pressure of the solution compared to the one of the pure solvent. This unbalance originates a temperature difference between the thermistors, which is proportionally recorded as a difference of resistance (ΔR) by the Wheatstone bridge (WB) of the osmometer [20].

The osmometer signals were recorded and the osmotic coefficient (ϕ) in each sample was calculated using equation (2).

$$\phi = \frac{\Delta R \cdot \nu_{\mathrm{ref}}}{k \cdot m \cdot \nu} \tag{2}$$

where ΔR is the osmometer signal, k is the slope of a reference line (ΔR vs m) unique to each equipment and determined with binary aqueous solutions of sodium chloride (NaCl), m is salt molality, and ν_{ref} and ν are the total number of ions into which one molecule of the reference salt ($\nu_{\mathrm{ref}} = 2$) and of the organic salt ($\nu = 3$ or 4) dissociate, respectively.

Then, the activity (a) was calculated based on the osmotic coefficients and using equation (3) [21].

$$a = \exp(-\phi \cdot M \cdot \nu \cdot m) \tag{3}$$

where M is the molar mass of the solvent (for water: $M = 18\ 02\ \mathrm{g \cdot mol^{-1}}$).

To determine the vapour pressure (p) of each binary solution, the following equation was iteratively solved [21,34]:

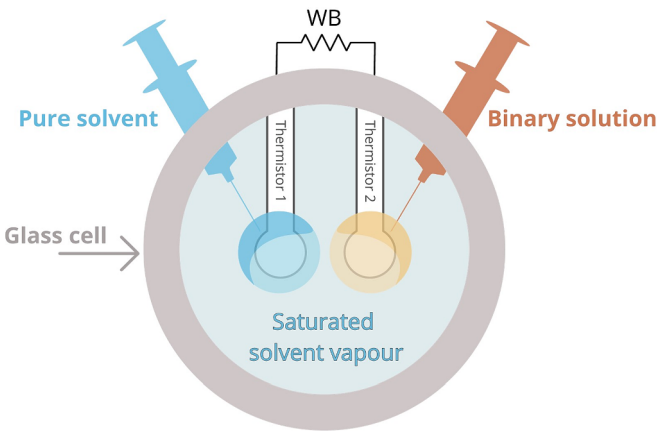

Fig. 1. Simplified schematic representation of the used vapour pressure osmometer (VPO), which contains a glass cell with saturated solvent vapour and two thermistors connected by a Wheatstone bridge (WB).

$$\ln(a) = \ln\left(\frac{p}{p^*}\right) + (B_S - V_S^*)(p - p^*)/(RT) \tag{4}$$

where p and p^* are the vapour pressures of the solution and of pure solvent, respectively, B_S is the second virial coefficient, V_S^* is the molar volume of the pure solvent, T is absolute temperature and R is the ideal gas constant (8.314 $\mathrm{J \cdot mol^{-1} \cdot K^{-1}}$). For water, at 313.15 K: $B_S = -9.701 \cdot 10^{-4}\ \mathrm{m^3 \cdot mol^{-1}}$ [35], $V_S^* = 1\ 8157 \cdot 10^{-5}\ \mathrm{m^3 \cdot mol^{-1}}$ [36] and $p^* = 7368\ 2\ \mathrm{Pa}$ (calculated using Antoine's equation [35,37]).

2.5.1. Extended Pitzer Model of Archer for the osmotic coefficients

In this work, the Extended Pitzer Model of Archer [16,17] was applied to describe the osmotic coefficients (ϕ). Therefore, these were considered as a function of a Debye-Hückel term (f^{ϕ}) and of the second (B_{MX}^{ϕ}) and third virial coefficients (C_{MX}^{ϕ}), as equation (5) shows [11].

$$\phi - 1 = |z_M \cdot z_X| \cdot f^{\phi} + m \cdot \left(\frac{2\nu_M \nu_X}{\nu_M + \nu_X}\right) \cdot B_{\mathrm{MX}}^{\phi} + m^2 \cdot \left(\frac{2\nu_M^{1.5}\nu_X^{1.5}}{\nu_M + \nu_X}\right) \cdot C_{\mathrm{MX}}^{\phi} \tag{5}$$

where z_i is the electronic charge and ν_i is the stoichiometric number of each salt ion, with $i = \mathrm{M}$ for the cation and $i = \mathrm{X}$ for the anion. B_{MX}^{ϕ} is a parameter which accounts for binary ion-ion interactions while C_{MX}^{ϕ} describes the ternary ones [38].

The Debye-Hückel term (f^{ϕ}) was calculated using [11]:

$$f^{\phi} = -A_{\phi} \cdot \frac{I^{0.5}}{1 + b \cdot I^{0.5}} \tag{6}$$

where A_{ϕ} is the Debye-Hückel parameter for the osmotic coefficients, b is a universal parameter equal to 1.2 $\mathrm{kg^{0.5} \cdot mol^{-0.5}}$ [11], and I stands for the ionic strength (in $\mathrm{mol \cdot kg^{-1}}$).

The Debye-Hückel parameter for the osmotic coefficients was calculated using the theoretical expression of equation (7), and it was found to be equal to 0.4024 $\mathrm{kg^{0.5} \cdot mol^{-0.5}}$, which agrees with data available in literature for these conditions [11].

$$A_{\phi} = \frac{1}{3} \cdot (2 \cdot \pi \cdot N_A \cdot \rho_w)^{0.5} \cdot \left(\frac{e^2}{4 \cdot \pi \cdot \epsilon_0 \cdot \epsilon_w \cdot k \cdot T}\right)^{1.5} \tag{7}$$

where N_A is Avogadro's number, ρ_w is the density of water (in $\mathrm{kg \cdot m^{-3}}$), e is the electronic charge, ϵ_0 is vacuum's permittivity, ϵ_w is the dielectric constant of water, k is the Boltzmann's constant and T is absolute temperature.

Following the work of Pitzer [11], an expression with three adjustable parameters (one extra compared to Debye-Hückel) was considered for the second virial coefficient (B_{MX}^{ϕ}), as equation (8) shows, since it allows to better describe electron pairing (mostly reported in 2–2 electrolytes [11]). This third ion-interaction parameter refers to the equilibrium constant of association and is typically negative.

$$B_{\mathrm{MX}}^{\phi} = \beta_{\mathrm{MX}}^{(0)} + \beta_{\mathrm{MX}}^{(1)} \cdot \exp(-\alpha_1 \cdot I^{0.5}) + \beta_{\mathrm{MX}}^{(2)} \cdot \exp(-\alpha_2 \cdot I^{0.5}) \tag{8}$$

where $\beta_{\mathrm{MX}}^{(0)}$, $\beta_{\mathrm{MX}}^{(1)}$, $\beta_{\mathrm{MX}}^{(2)}$, α_1 and α_2 are adjustable parameters. In this work, to reduce the number of parameters, α_1 and α_2 were considered as 1.4 $\mathrm{kg^{0.5} \cdot mol^{-0.5}}$ and 12 $\mathrm{kg^{0.5} \cdot mol^{-0.5}}$, respectively, following other works on electrolytes [11,23,39–41].

On the other hand, the third virial coefficient $\left(C_{\mathrm{MX}}^{\phi}\right)$ was calculated following a modification by Archer [16,17], which includes a dependence of this parameter with ionic strength, as equation (9) shows.

$$C_{\mathrm{MX}}^{\phi} = C^{(0)} + C^{(1)} \cdot \exp(-\alpha_3 \cdot I^{0.5}) \tag{9}$$

where $C^{(0)}$, $C^{(1)}$ and α_3 are adjustable parameters. In this work, also to ease parameterization, α_3 was considered as 2.5 $\mathrm{kg^{0.5} \cdot mol^{-0.5}}$, following other works on this topic [23,39,42,43].

2.5.2. Extended Pitzer Model of Archer for the mean activity coefficients

By definition, the mean molal activity coefficient ($\gamma_{\pm}$) of a salt is calculated as [11]:

$$\ln(\gamma_{\pm}) = \frac{\nu_M \ln(\gamma_M) + \nu_X \ln(\gamma_X)}{\nu_M + \nu_X} \quad (10)$$

For a solution of a single MX salt, and following the work of Pitzer [11], equation (11) was used to determine the mean molal activity coefficients of the prepared samples.

$$\ln(\gamma_{\pm}) = |z_M \cdot z_X| \cdot f^{\gamma} + m \cdot \left(\frac{2\nu_M \nu_X}{\nu_M + \nu_X}\right) \cdot B^{\gamma}_{MX} + m^2 \cdot \left(\frac{2\nu_M^{1.5}\nu_X^{1.5}}{\nu_M + \nu_X}\right) \cdot C^{\gamma}_{MX} \quad (11)$$

where f^{γ}, B^{γ}_{MX} and C^{γ}_{MX} were determined using equations (12), (13), and (14), respectively [11].

$$f^{\gamma} = A_{\phi} \cdot \left[\frac{I^{0.5}}{1 + b \cdot I^{0.5}} + \frac{2}{b} \cdot \ln(1 + b \cdot I^{0.5})\right] \quad (12)$$

$$B^{\gamma}_{MX} = B^{\phi}_{MX} + \beta^{(0)}_{MX} + \beta^{(1)}_{MX} \cdot \frac{2}{\alpha_1^2 \cdot I} \cdot \left[1 - \left(1 + \alpha_1 \cdot I^{0.5}\right) \cdot \exp\left(\alpha_1 \cdot I^{0.5}\right)\right] + \beta^{(2)}_{MX} \cdot \frac{2}{\alpha_2^2 \cdot I} \cdot \left[1 - \left(1 + \alpha_2 \cdot I^{0.5}\right) \cdot \exp\left(\alpha_2 \cdot I^{0.5}\right)\right] \quad (13)$$

$$C^{\gamma}_{MX} = 1.5 \cdot C^{\phi}_{MX} \quad (14)$$

Then, the excess Gibbs free energies (G^E/RT) were determined using the calculated mean activity coefficients ($\gamma_{\pm}$) following equation (15) [11].

$$\frac{G^E}{RT} = (\nu_M + \nu_X) \cdot m \cdot [\ln(\gamma_{\pm}) + 1 - \phi] \quad (15)$$

3. Results and discussion

3.1. Density measurement and correlation

The obtained liquid densities (ρ), at 298.15 and 313.15 K and 0.1 MPa, for the prepared binary aqueous solutions of disodium tartrate ($C_4H_4Na_2O_6$), sodium potassium tartrate ($C_4H_4NaKO_6$), dipotassium tartrate ($C_4H_4K_2O_6$), trisodium citrate ($C_6H_5Na_3O_7$) and tripotassium citrate ($C_6H_5K_3O_7$) can be seen in Table S2, in the Supplementary Materials.

As Fig. 2 shows, citrate and potassium salts presented significantly higher liquid densities than tartrate and sodium salts, as already verified in other works [44–48], with the salt-anions having a more preponderant effect on density than the salt-cations. This fact is probably due to the generally larger polarizabilities of anions [49], which increase their influence on solvation and, consequently, on volume and density. Moreover, as expected, a decrease in temperature caused an increase in the liquid densities given a more tightly packed state of the particles at lower kinetic energies. The obtained liquid densities were compared with the available literature [48,50–54], as Figs. S3-S7, in the Supplementary Materials, show, and a general agreement was observed, validating the reported data.

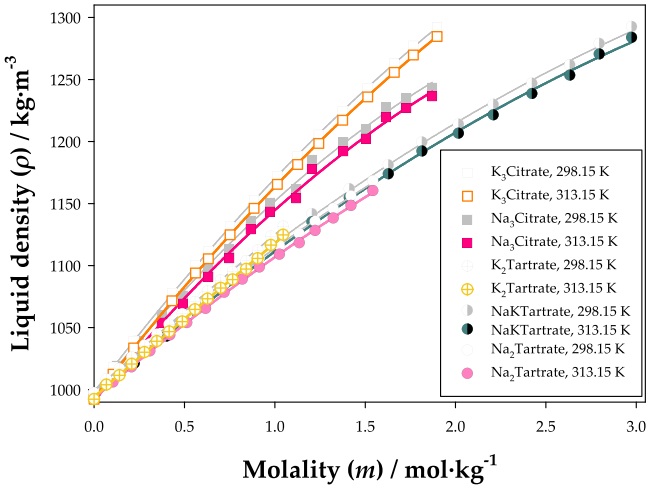

Fig. 2. Liquid density (ρ) with salt molality (m) for binary aqueous solutions of disodium tartrate (Na_2Tartrate), sodium potassium tartrate (NaKTartrate), dipotassium tartrate (K_2Tartrate), trisodium citrate (Na_3Citrate) and tripotassium citrate (K_3Citrate) at 298.15 and 313.15 K and 0.1 MPa.

The obtained liquid density data were fitted to second-degree polynomials in function of molality (m), as seen in equation (1). As Table 2 shows, very good fittings were attained for all binaries, particularly to what pertains tripotassium citrate, as evidenced by the high determination coefficients verified ($R^2 = 0.99996$),

3.2. VPO measurement and modelling

The obtained experimental osmotic coefficients (ϕ), activities (a), and vapour pressures (p), at 313.15 K and 0.1 MPa, for the binary aqueous solutions of organic salts can be observed in Table 3.

As anticipated, an increased concentration of electrolyte originated a decrease in the observed vapour pressure, *i.e.*, the vapour pressure of the solution (p) is lower than the one of the pure solvent (p^*), causing a negative difference of vapour pressure ($\Delta p = p - p^* < 0$). As Fig. 3 shows, citrate- and potassium-based salts presented higher absolute values of Δp than tartrate and sodium salts, hinting at a larger deviation from pure solvent state. This may be due to the larger valency of citrate salts compared to tartrates and to the stronger salting out character of potassium ions compared to the ones of sodium, as given by the Hofmeister series [55]. Therefore, the increased polarity of potassium- or citrate-based salts promotes a less random media and a larger deviation from the pure solvent state. Similarly to what was performed for liquid densities, second-degree polynomials were used to portray the influence of molality (m) on Δp, and their obtained adjustable parameters and determination coefficients (R^2) can be seen in Table S3, in the Supplementary Materials.

As Fig. 4 illustrates, sodium-based salts obtained lower values of osmotic coefficients (ϕ) compared to the ones containing the potassium cation, which is commonly reported in literature [56–59] (with the exception of $H_2PO_4^-$ salts [59,60]), and citrate salts presented a more pronounced local minimum (at approximately $m = 0.5$ mol·kg^{-1}). The osmotic coefficients of the aqueous solutions of K_2Tartrate were compared with literature [53] and, even though the general behaviour was similar, they were found to be slightly higher than expected, as Fig. S8, in the Supplementary Materials shows. This gap could be due to the high sensitivity of vapour pressure osmometers. Nevertheless, the Extended Pitzer Model of Archer satisfactorily modelled the effect of molality on the osmotic coefficients for all studied binaries, and the obtained adjustable parameters ($\beta^{(0)}, \beta^{(1)}, \beta^{(2)}, C^{(0)}$ and $C^{(1)}$) are shown in Table S4, in the Supplementary Materials, together with the respective standard deviations.

While all other systems presented negative values for the $\beta^{(2)}$ parameter, dipotassium tartrate (K_2Tartrate) obtained a positive one ($\beta^{(2)} = 34.150$). This parameter is related to the association constant of electrolytes and is typically negative, so a positive value suggests the absence of ion pairing. Nevertheless, one cannot forget that the addition of this parameter aims to enhance data fitting while avoiding more complex terms, which generally consider the ion pair as a different species [11]. Therefore, its interpretation is always dependent on the values chosen for other parameters (such as b), becoming more trustworthy at higher temperatures, in which ion pairing is more preponderant [61]. Thus, even though the Extended Pitzer Model of Archer provided a particularly good description of the osmotic coefficients, novel parameterisation alternatives are required to foster a deeper

Table 2
Obtained adjustable parameters for the second-degree polynomials of liquid density (ρ) with salt molality (m) for binary aqueous solutions of different organic salts at $T = 298\ 15$ and 313.15 K and $P = 0\ 1$ MPa, with respective determination coefficients (R^2)[a,b].

Salt	T/K	ρ_0 / kg·m ^{3}	ρ_1 / kg^2·m ^{3}·mol ^{1}	ρ_2 / kg^3·m ^{3}·mol ^{2}	R^2
Disodium tartrate	298.15	998.8	131	4.88	0.9995
	313.15	994.0	128	4.14	0.9994
Sodium potassium tartrate	298.15	999.4	129	10.7	0.9995
	313.15	994.0	128	10.8	0.9994
Dipotassium tartrate	298.15	997.9	128	11.9	0.9997
	313.15	993.0	125	11.3	0.9997
Trisodium citrate	298.15	995.8	181	24.9	0.9982
	313.15	990.7	178	23.7	0.9982
Tripotassium citrate	298.15	998.2	191	19.2	0.99996
	313.15	993.0	189	18.8	0.99996

[a] $\rho = \rho_0 + \rho_1 \cdot m + \rho_2 \cdot m^2$, where m is salt molality and ρ_0, ρ_1, and ρ_2 are adjustable parameters.
[b] The standard measurement uncertainties (u) are: $u(\rho) = 0\ 25$ kg·m ^{3}, $u(T) = 0\ 1$ K and $u(P) = 2$ kPa.

Table 3
Experimental osmotic coefficients (ϕ), activities (a), and vapour pressures (p) with salt molality (m) for binary aqueous solutions of different organic salts, at $T = 313\ 15$ K and $P = 0\ 1$MPa.[a]

m / mol·kg ^{1}	ϕ	a	p / kPa	m / mol·kg ^{1}	ϕ	a	p/ kPa
Disodium tartrate							
0.104	0.857	0.9952	7.333	0.915	0.671	0.9673	7.127
0.207	0.802	0.9911	7.302	1.025	0.668	0.9636	7.100
0.309	0.774	0.9872	7.273	1.136	0.665	0.9600	7.073
0.420	0.739	0.9834	7.245	1.223	0.669	0.9567	7.049
0.513	0.725	0.9801	7.221	1.324	0.669	0.9532	7.023
0.617	0.706	0.9767	7.196	1.422	0.675	0.9495	6.995
0.720	0.693	0.9734	7.171	1.543	0.685	0.9445	6.958
0.820	0.680	0.9703	7.149				
Sodium potassium tartrate							
0.223	0.829	0.9901	7.295	1.814	0.726	0.9313	6.860
0.399	0.758	0.9838	7.248	2.016	0.746	0.9219	6.792
0.610	0.731	0.9762	7.192	2.209	0.760	0.9132	6.727
0.808	0.708	0.9696	7.143	2.423	0.777	0.9032	6.653
1.013	0.697	0.9626	7.092	2.632	0.788	0.8939	6.584
1.205	0.690	0.9560	7.043	2.796	0.800	0.8861	6.527
1.412	0.697	0.9481	6.985	2.975	0.816	0.8770	6.460
1.629	0.712	0.9392	6.919				
Dipotassium tartrate							
0.068	0.955	0.9965	7.342	0.628	0.736	0.9753	7.186
0.140	0.910	0.9931	7.317	0.700	0.732	0.9727	7.166
0.208	0.883	0.9901	7.295	0.766	0.731	0.9702	7.148
0.279	0.843	0.9874	7.275	0.842	0.728	0.9674	7.127
0.347	0.804	0.9850	7.257	0.905	0.729	0.9650	7.109
0.415	0.773	0.9828	7.241	0.978	0.732	0.9620	7.088
0.488	0.753	0.9803	7.223	1.046	0.733	0.9594	7.068
0.558	0.740	0.9779	7.205				
Trisodium citrate							
0.126	0.665	0.9940	7.324	1.117	0.561	0.9558	7.042
0.246	0.518	0.9909	7.301	1.204	0.576	0.9513	7.008
0.373	0.476	0.9873	7.274	1.378	0.604	0.9417	6.938
0.492	0.470	0.9835	7.246	1.503	0.625	0.9345	6.884
0.632	0.482	0.9783	7.208	1.615	0.646	0.9276	6.833
0.748	0.500	0.9734	7.172	1.728	0.666	0.9204	6.780
0.866	0.519	0.9681	7.133	1.871	0.703	0.9096	6.705
0.974	0.536	0.9631	7.095				
Tripotassium citrate							
0.141	0.904	0.9909	7.301	1.274	0.710	0.9369	6902.37
0.279	0.727	0.9855	7.261	1.370	0.727	0.9307	6856.41
0.426	0.661	0.9799	7.220	1.526	0.752	0.9206	6781.80
0.584	0.634	0.9736	7.174	1.640	0.766	0.9135	6729.28
0.696	0.632	0.9688	7.138	1.784	0.788	0.9037	6656.83
0.821	0.645	0.9625	7.091	1.928	0.810	0.8935	6581.74
0.981	0.666	0.9540	7.028	2.073	0.850	0.8808	6487.67
1.105	0.687	0.9467	6.975				

[a]The standard measurement uncertainties (u) are: $u(m) = 2{\cdot}10^{-3}$ mol·kg ^{1}, $u(\phi) = 8{\cdot}10^{-3}$, $u(a) = 3{\cdot}10^{-2}$, $u(p) = 1$ Pa, $u(T) = 0\ 1$ K and $u(P) = 2$ kPa.

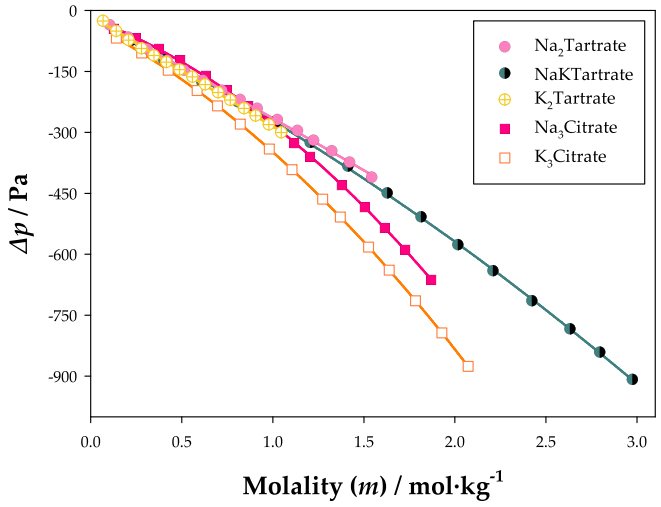

Fig. 3. Difference of vapour pressure (Δp) with salt molality (m) for binary aqueous solutions of disodium tartrate (Na_2Tartrate), sodium potassium tartrate (NaKTartrate), dipotassium tartrate (K_2Tartrate), trisodium citrate (Na_3Citrate) and tripotassium citrate (K_3Citrate) at 313.15 K and 0.1 MPa.

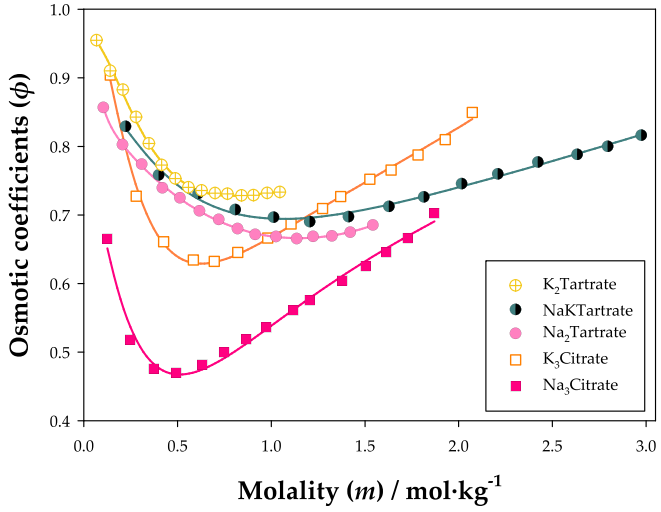

Fig. 4. Experimental osmotic coefficients (ϕ) with salt molality (m) and respective thermodynamic modelling using the Extended Pitzer Model of Archer for binary aqueous solutions of different organic salts at 313.15 K and 0.1 MPa.

interpretation of the physical meaning of the parameters in future works. For example, solubility data at high ionic strength have been used to estimate Pitzer parameters [15], computational chemistry has been used to parameterise other thermodynamic models [62], and there is theoretical support for the proportionality of the α_2 parameter with the Debye-Hückel constant [11,63].

After having applied the Extended Pitzer Model of Archer in the modelling of the experimental osmotic coefficients, the mean molal activity coefficients ($\gamma_\pm$) and the excess Gibbs free energies $\left(\frac{G^E}{RT}\right)$ were calculated using equations (11) and (15), respectively, as shown in Table 4.

As Fig. 5 shows, potassium-based salts, which also presented higher osmotic coefficients, obtained higher mean molal activity coefficients than the respective sodium salts and, consequently, lower deviations from an ideal solution ($\gamma_\pm = 1$). Moreover, tartrates achieved significantly higher values of osmotic and mean molal activity coefficients than the respective citrates, and this gap may be explained by the larger

Table 4
Calculated mean molal activity coefficients ($\gamma_\pm$) and excess Gibbs free energies $\left(\frac{G^E}{RT}\right)$ with salt molality (m) for binary aqueous solutions of different organic salts at T = 313 15 K and P = 0 1 MPa.

m / mol·kg ^{1}	$\gamma_\pm$	$\frac{G^E}{RT}$	m / mol·kg ^{1}	$\gamma_\pm$	$\frac{G^E}{RT}$
Disodium tartrate					
0.104	0.4380	0.21	0.915	0.2811	2.58
0.207	0.3855	0.47	1.025	0.2775	2.93
0.309	0.3524	0.76	1.136	0.2751	3.27
0.420	0.3278	1.08	1.223	0.2739	3.54
0.513	0.3129	1.36	1.324	0.2732	3.85
0.617	0.3006	1.67	1.422	0.2730	4.15
0.720	0.2918	1.99	1.543	0.2734	4.53
0.820	0.2855	2.29			
Sodium potassium tartrate					
0.223	0.4058	0.49	1.814	0.3402	4.38
0.399	0.3630	0.94	2.016	0.3463	4.85
0.610	0.3379	1.48	2.209	0.3523	5.30
0.808	0.3279	1.98	2.423	0.3590	5.79
1.013	0.3249	2.49	2.632	0.3658	6.28
1.205	0.3261	2.95	2.796	0.3712	6.66
1.412	0.3297	3.44	2.975	0.3771	7.07
1.629	0.3350	3.95			
Dipotassium tartrate					
0.068	0.8600	0.02	0.628	0.8303	0.15
0.140	0.8228	0.05	0.700	0.8603	0.25
0.208	0.7973	0.06	0.766	0.8917	0.36
0.279	0.7805	0.07	0.842	0.9308	0.50
0.347	0.7740	0.06	0.905	0.9656	0.64
0.415	0.7765	0.04	0.978	1.0068	0.81
0.488	0.7879	0.01	1.046	1.0454	0.97
0.558	0.8062	0.07			
Trisodium citrate					
0.126	0.2424	0.54	1.117	0.1635	6.13
0.246	0.1872	1.20	1.204	0.1656	6.63
0.373	0.1649	1.92	1.378	0.1694	7.64
0.492	0.1571	2.59	1.503	0.1719	8.38
0.632	0.1549	3.39	1.615	0.1741	9.04
0.748	0.1558	4.04	1.728	0.1761	9.72
0.866	0.1578	4.71	1.871	0.1784	10.58
0.974	0.1602	5.31			
Tripotassium citrate					
0.141	0.5895	0.24	1.274	1.0895	1.91
0.279	0.5903	0.30	1.370	1.1338	2.19
0.426	0.6324	0.20	1.526	1.1997	2.63
0.584	0.7089	0.06	1.640	1.2443	2.94
0.696	0.7719	0.31	1.784	1.2976	3.34
0.821	0.8456	0.62	1.928	1.3485	3.73
0.981	0.9376	1.06	2.073	1.3984	4.11
1.105	1.0055	1.42			

[a] The standard measurement uncertainties (u) are: $u(T)$ = 0 1 K and $u(P)$ = 2 kPa.

absolute charge of the latter ($|z| = 3e > 2e$) and by the consequent larger number of total ions ($\nu = 4 > 3$), which increase the ionic strength of dissolved electrolytes for the same concentration of molecular salt, contributing to a larger decrease in vapour pressure and to a larger deviation from ideality for citrates.

In Fig. 6, it can be noticed that sodium-based salts presented a decreasingly negative excess Gibbs free energy with increasing molality, while the opposite was observed for the ones based on potassium. Therefore, there is a thermodynamic driving force for spontaneous solubilisation to occur in sodium-based salts, while potassium salts tend to become less soluble in water at higher salt molality. This trend was already projected given the substantial growth observed for activity coefficients with salt molality for potassium-salts in Fig. 5, which contrasts with a practically constant behaviour for the ones based on sodium.

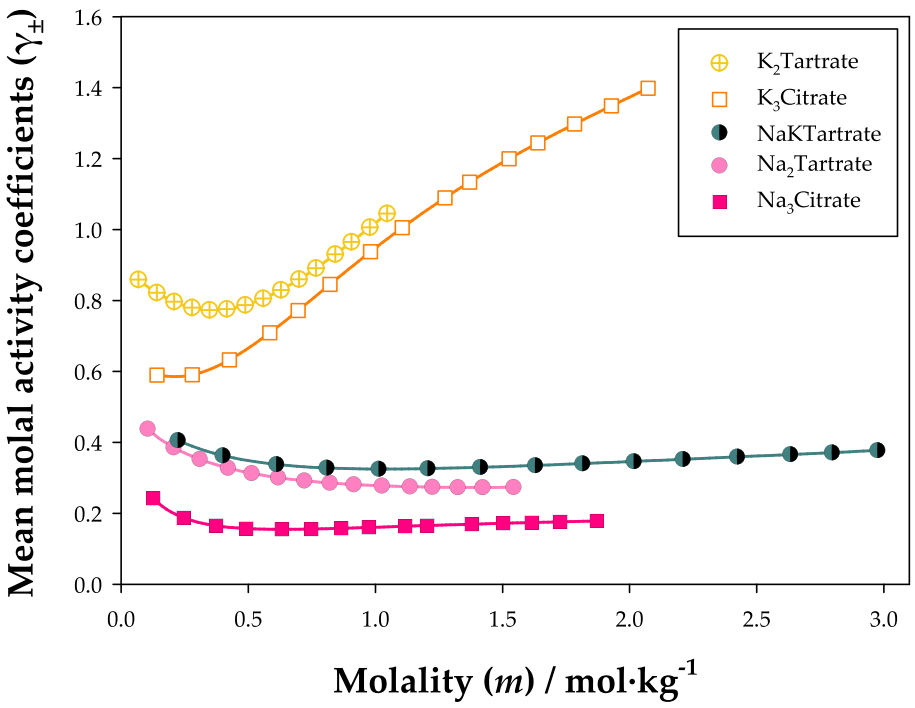

Fig. 5. Calculated mean molal activity coefficients ($\gamma_\pm$) with salt molality (m) for binary aqueous solutions of different organic salts at 313.15 K and 0.1 MPa.

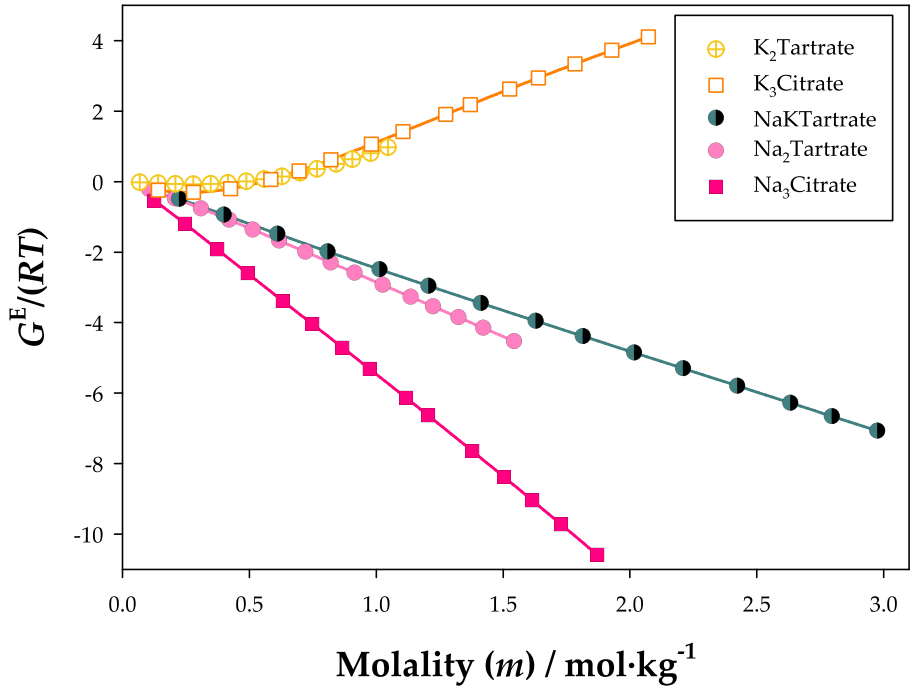

Fig. 6. Calculated excess Gibbs free energy (G^E/RT) with salt molality (m) for binary aqueous solutions of different organic salts at 313.15 K and 0.1 MPa.

4. Conclusions

Vapour pressure osmometry (VPO) and liquid density measurements are essential for the development and tuning of thermodynamic models, but data concerning binary aqueous solutions of organic salts are scarce, so the implementation of these compounds in greener chemical processes has been limited.

The liquid density measurements, performed at 298.15 and 313.15 K and 0.1 MPa for five binary aqueous solutions of the organic salts disodium tartrate, sodium potassium tartrate, dipotassium tartrate, trisodium citrate and tripotassium citrate, showed a second-degree dependence with salt molality, with potassium- and citrate-based salts achieving higher densities. Moreover, as expected, lower temperatures caused an increase in liquid density due to a more tightly packed state of the particles at lower kinetic energies.

Osmotic coefficients were successfully determined from VPO measurements and modelled using the Extended Pitzer Model of Archer, which also yielded the mean molal activity coefficients and excess Gibbs

free energies of each solution. Salts composed of potassium and tartrate attained larger values of the activity coefficients, hinting at a more ideal solution behaviour. Nevertheless, it was found that the values of the adjustable parameters of this thermodynamic model were too sensitive to the initial considerations (assumed values of other parameters), for which novel parameterisation methodologies are needed (*e.g.*, using solubility data, correlating parameters, or using computational chemistry).

CRediT authorship contribution statement

Pedro Velho: Writing – original draft, Writing – review & editing, Validation, Methodology, Investigation, Formal analysis, Conceptualization. **Eduardo Sousa:** Writing – review & editing, Visualization, Investigation, Formal analysis. **Eugenia A. Macedo:** Writing – review & editing, Supervision, Conceptualization.

Declaration of competing interest

The authors declare that they have no known competing financial interests or personal relationships that could have appeared to influence the work reported in this paper.

Data availability

Data will be made available on request.

Acknowledgements

This work was supported by national funds through FCT/MCTES (PIDDAC): LSRE-LCM, UIDB/50020/2020 (DOI: 10.54499/UIDB/50020/2020) and UIDP/50020/2020 (DOI: 10.54499/UIDP/50020/2020); and ALiCE, LA/P/0045/2020 (DOI: 10.54499/LA/P/0045/2020). Pedro Velho is grateful for the funding support from FCT [2021.06626.BD].

Appendix A. Supplementary data

Supplementary data to this article can be found online at https://doi.org/10.1016/j.jct.2024.107287.

References

[1] P. Anastas, N. Eghbali, Green chemistry: principles and Practice, Chem. Soc. Rev. 39 (2010) 301–312.
[2] A. Anderko, P. Wang, M. Rafal, Electrolyte solutions: from thermodynamic and transport property models to the simulation of industrial processes, Fluid Phase Equilib. 194–197 (2002) 123–142.
[3] G.M. Kontogeorgis, B. Maribo-Mogensen, K. Thomsen, The debye-hückel theory and its importance in modeling electrolyte solutions, Fluid Phase Equilib. 462 (2018) 130–152.
[4] G.M. Kontogeorgis, Association theories for complex thermodynamics, Chem. Eng. Res. Des. 91 (2013) 1840–1858.
[5] P. Velho, X. Liang, E.A. Macedo, E. Gomez, G.M. Kontogeorgis, Towards a predictive cubic plus association equation of state, Fluid Phase Equilib. 540 (2021) 113045.
[6] B. Gonzalez, N. Calvar, A. Domínguez, E.A. Macedo, Osmotic coefficients of aqueous solutions of four ionic liquids at T = (313.15 and 333.15) K, J. Chem. Thermodyn. 40 (2008) 1346–1351.
[7] L. Sun, Q. Lei, B. Peng, G.M. Kontogeorgis, X. Liang, An analysis of the parameters in the debye-hückel theory, Fluid Phase Equilib. 556 (2022) 113398.
[8] P. Debye, E. Hückel, Zur theorie der elektrolyte. i. Gefrierpunktserniedrigung und verwandte erscheinungen, Phys. Z 24 (1923) 185–206.
[9] L. Blum, Mean spherical model for Asymmetric electrolytes: I. Method of Solution, *Mol. Phys.* 30 (1975) 1529–1535.
[10] L. Blum, J.S.M. Høye, Spherical model for Asymmetric electrolytes. 2. thermodynamic properties and the pair Correlation function, J. Phys. Chem. 81 (1977) 1311–1316.
[11] K.S. Pitzer, Activity coefficients in electrolyte solutions, CRC Press, 1991.
[12] D. Rowland, E. Königsberger, G. Hefter, P.M. May, Aqueous electrolyte solution modelling: some limitations of the pitzer equations, Appl. Geochem. 55 (2015) 170–183.
[13] K.S. Pitzer, Thermodynamics of electrolytes. I. Theoretical basisand general equations, J. Phys. Chem. 77 (1973) 268–277.
[14] M.C. Simoes, K.J. Hughes, D.B. Ingham, L. Ma, M. Pourkashanian, Estimation of the pitzer Parameters for 1–1, 2–1, 3–1, 4–1, and 2–2 single electrolytes at 25 °C, J. Chem. Eng. Data 61 (2016) 2536–2554.
[15] C.F. Weber, Calculation of pitzer Parameters at high ionic strengths, Ind. Eng. Chem. Res. 39 (2000) 4422–4426.
[16] D.G. Archer, Thermodynamic properties of the NaBr+H2O system, J. Phys. Chem. Ref. Data 50 (1991) 509–555.
[17] D.G. Archer, Thermodynamic properties of the NaCI + H20 system II. thermodynamic properties of NaCI(aq), NaCI·2H2O(cr), and Phase Equilibria, J. Phys. Chern. Ref. Data 21 (1992) 793–829.
[18] K. Nasirzadeh, R. Neueder, W. Kunz, Vapor pressures, osmotic and activity coefficients of electrolytes in protic solvents at different temperatures. 2. lithium bromide in ethanol, J. Solution Chem. 33 (2004) 1429–1446.
[19] N. Calvar, B. Gonzalez, A. Domínguez, E.A. Macedo, Vapour pressures and osmotic coefficients of binary mixtures of 1-ethyl-3-methylimidazolium ethylsulfate and 1-ethyl-3-methylpyridinium ethylsulfate with alcohols at T = 323.15 K, J. Chem. Thermodyn. 41 (2009) 1439–1445.
[20] K. Wysoczanska, N. Calvar, E.A. Macedo, (Vapor + liquid) equilibria of alcohol + 1-methyl-1-propylpiperidinium triflate ionic liquid: VPO measurements and modeling, J. Chem. Thermodyn. 97 (2016) 183–190.
[21] K. Nasirzadeh, R. Neueder, W. Kunz, Vapor pressures, osmotic and activity coefficients for (LiBr + acetonitrile) between the temperatures (298.15 and 343.15) K, J. Chem. Thermodyn. 36 (2004) 511–517.
[22] K. Nasirzadeh, R. Neueder, W. Kunz, Vapor pressures and osmotic coefficients of aqueous LiOH solutions at temperatures ranging from 298.15 to 363.15 K, Ind. Eng. Chem. Res. 44 (2005) 3807–3814.
[23] S.L. Clegg, J.A. Rard, D.G. Miller, Isopiestic determination of the osmotic and activity coefficients of NaCl + SrCl2 + H2O at 298.15 K and representation with an extended ion-Interaction model, J. Chem. Eng. Data 50 (2005) 1162–1170.
[24] C.S. Rebelo, P. Velho, E.A. Macedo, Partition studies of resveratrol in low-impact ATPS for food supplementation, Ind. Eng. Chem. Res. (2023).
[25] M.M. Pereira, S.N. Pedro, M.V. Quental, A. Mohamadou, J.A.P. Coutinho, M. G. Freire, Integrated approach to Extract and purify proteins from honey by ionic liquid-based three-phase Partitioning, ACS Sustainable Chem. Eng. 10 (2022) 9275–9281.
[26] J.H. Santos, F.A. Silva, S.P.M. Ventura, J.A.P. Coutinho, R.L. Souza, C.M.F. Soares, A.S. Lima, Ionic liquid-based aqueous biphasic systems as a versatile tool for the recovery of antioxidant compounds, Biotechnol. Prog. 31 (2014) 70–77.
[27] K.S. Nascimento, P.A.J. Rosa, K.S. Nascimento, B.S. Cavada, A.M. Azevedo, M. R. Aires-Barros, Partitioning and recovery of Canavalia brasiliensis lectin by aqueous two-phase systems using design of experiments methodology, Sep. Purif. Technol. 75 (2010) 48–54.
[28] V.H. Nagaraja, R. Iyyaswami, Aqueous two phase partitioning of fish proteins: partitioning studies and ATPS evaluation, J Food Sci Technol. 52 (2015) 3539–3548.
[29] R.C. Assis, A.B. Mageste, L.R. Lemos, R.M. Orlando, G.D. Rodrigues, Application of aqueous two-phase systems for the extraction of pharmaceutical compounds from water samples, J. Mol. Liq. 301 (2020) 112411.
[30] P. Velho, E. Sousa, E.A. Macedo, Extraction of salicylic acid using sustainable ATPSs and respective immobilization as API-IL at small pilot-scale, J. Chem. Eng. Data (2023).
[31] P. Li, X. Li, Y. Guo, C. Li, Y. Hou, H. Cui, R. Zhang, Z. Huang, Y. Zhao, Q. Li, B. Dong, C. Zhi, Highly thermally/electrochemically stable I /I3 bonded organic salts with high I content for long-life Li–I2 batteries, Adv. Energy Mater. 12 (2022) 2103648.
[32] S. Clark, A.R. Mainar, E. Iruin, L.C. Colmenares, J.A. Blazquez, J.R. Tolchard, Z. Jusys, B. Horstmann, Designing aqueous organic electrolytes for zinc-air batteries: method, simulation, and validation, Adv. Energy Mater. 10 (2020) 1903470.
[33] W. Gildseth, A. Habenschuss, F.H. Spedding, Precision measurements of densities and thermal dilation of water between 5 and 80 C, J. Chem. Eng. Data 17 (1972) 402–409.
[34] N. Calvar, A. Domínguez, E.A. Macedo, Activity and osmotic coefficients of Binary mixtures of NTf2 - ionic liquids with a Primary alcohol, J. Chem. Eng. Data 61 (2016) 4123–4130.
[35] B.E. Poling, J.M. Prausnitz, J.P. O'Connell, The properties of gases and liquids, McGraw-Hill, 2001.
[36] J.H. Keenan, F.G. Keyes, P.G. Hill, J.G. Moore, Steam tables: thermodynamic properties of water including vapour, liquid and solid phases, Wiley-Interscience, 1969.
[37] M.C. Antoine, Tensions des vapeurs: nouvelle relation entre les tensions et les temperatures, C. R. Acad. Sci. Paris 107 (681–684) (1888), pp. 778–780, 836–837.
[38] C.-C. Chen, H.I. Britt, J.F. Boston, L.B. Evans, Extension and application of the pitzer equation for vapor-liquid equilibrium of aqueous electrolyte systems with molecular solutes, AICHE J. 25 (1979) 820–831.
[39] G.A. Iglesias-Silva, Comparison among pitzer-type models for the osmotic and activity coefficients of strong electrolyte solutions at 298.15 K, Ind. Eng. Chem. Res. 50 (2011) 10894–10901.
[40] J.A. Rard, S.L. Clegg, Isopiestic determination of the osmotic and activity coefficients of {zH2SO4+ (1 z)MgSO4}(aq) at T = 298.15 K. II. results for z = (0.43040, 0.28758, and 0.14399) and analysis with pitzer's model, J. Chem. Thermodyn. 31 (1999) 399–429.
[41] D.A. Palmer, J.A. Rard, S.L. Clegg, Isopiestic determination of the osmotic and activity coefficients of Rb2SO4(aq) and Cs2SO4(aq) at T = (298.15 and 323.15) K,

and representation with an extended ion interaction (pitzer) model, J. Chem. Thermodyn. 34 (2002) 63–102.
[42] J. Macaskill, R. Robinson, R. Bates, Osmotic coefficients and activity coefficients of guanidinium chloride in concentrated aqueous solutions at 25 ℃, J. Chem. Eng. Data 22 (1977) 411–412.
[43] R. Ninkovic, J. Miladinovic, M. Todorovic, S. Grujic, J.A. Rard, Osmotic and activity coefficients of the [x ZnCl2+(1–x)ZnSO4](aq) system at 298.15 K, J. Solution Chem. 36 (2007) 405–435.
[44] A. Delanney, A. Ledoux, L. Estel, G.C. Villegas, C. Baret, Density and viscosity of potassium and sodium glycinate solutions, J. Chem. Eng. Data 68 (2023) 1267–1278.
[45] Romankiw, L.A.; Chou, I.M. Densities of aqueous sodium chloride, potassium chloride, magnesium chloride, and calcium chloride binary solutions in the concentration range 0.5-6.1 m at 25, 30, 35, 40, and 45 ℃. *J. Chem. Eng. Data* **1983**, 28, 300-305.
[46] A. Barani, M. Pirdashti, A.A.D. Rostami, Viscosity, Refractive index, and excess properties of Binary and Ternary solutions of poly(ethylene glycol), water, and dipotassium Tartrate at 298.15 K and atmospheric pressure, J. Chem. Eng. Data 63 (2017) 127–137.
[47] M. Pirdashti, K. Movagharnejad, A.A. Rostami, P. Akbarpour, M. Ketabi, Liquid-liquid equilibrium data, viscosities, densities, conductivities, and Refractive indexes of aqueous mixtures of poly(ethylene glycol) with Trisodium citrate at different pH, J. Chem. Eng. Data 60 (2015) 3423–3429.
[48] R. Sadeghi, F. Ziamajidi, Thermodynamic properties of tripotassium citrate in water and in aqueous solutions of polypropylene oxide 400 over a range of temperatures, J. Chem. Eng. Data 52 (2007) 1753–1759.
[49] M.K. Satti, M. Nayyer, M. Alshamrani, M. Kaleem, A. Salawi, A.Y. Safhi, A. Alsalhi, F.Y. Sabei, A.S. Khan, N. Muhammad, Synthesis, Characterization, and investigation of novel ionic liquid-based tooth bleaching gels: a step towards safer and cost-effective cosmetic dentistry, Molecules 28 (2023) 3131.
[50] M.T. Zafarani-Moattar, S. Hosseinzadeh, Refractive index, viscosity, density, and speed of sound of aqueous sodium Tartrate solutions at Various temperatures, J. Chem. Eng. Data 51 (2006) 1190–1193.
[51] Apelblat, A.; Manzurola, E. Volumetric properties of aqueous solutions of disodium tartrate and dipotassium-tartrate at temperatures from 278.15 K to 343.15 K and molalities (0.1, 0.5, and 1.0) mol·kg-1. *J. Chem. Thermodyn.* **2001**, 33, 1157-1168.
[52] A. Apelblat, E. Manzurola, Apparent molar volumes of organic acids and salts in water at 298.15 K, Fluid Phase Equilib. 60 (1990) 157–171.
[53] M.T. Zafarani-Moattar, B. Asadzadeh, Vapor-liquid equilibria, density, speed of sound, and viscosity of aqueous dipotassium Tartrate solutions at T = (298.15, 308.15, and 318.15) K, J. Chem. Eng. Data 53 (2008) 1000–1006.
[54] P. Sharma, S. Sharma, M. Sharma, Effect of trisodium citrate dihydrate on thermophysical properties of saccharides in aqueous media at different temperatures: volumetric and acoustic properties, Chem. Therm. Therm. Anal. 5 (2022) 100051.
[55] F. Hofmeister, On the understanding of the effects of salts, Naunyn-Schmiedeberg's Arch. Pharmacol. 24 (1888) 247–260.
[56] J.I. Partanen, Mean activity coefficients and osmotic coefficients in dilute aqueous sodium or potassium chloride solutions at temperatures from (0 to 70) °C, J. Chem. Eng. Data 61 (2016) 286–306.
[57] O.D. Bonner, Osmotic and activity coefficients of sodium chloride-sorbitol and potassium chloride-sorbitol solutions at 25°C, J. Solution Chem. 11 (1982) 315–324.
[58] H.F. Holmes, J.M. Simonson, R.E. Mesmer, Aqueous solutions of the mono- and di-hydrogenphosphate salts of sodium and potassium at elevated temperatures, Isopiestic Results. *J. Chem. Thermodyn.* 32 (2000) 77–96.
[59] M.E. Guendouzi, A. Benbiyi, Thermodynamic properties of binary aqueous solutions of orthophosphate salts, sodium, potassium and ammonium at T = 298.15K, Fluid Phase Equilib. 369 (2014) 68–85.
[60] G. Scatchard, R.C.I. Breckenridge, I.I. Solutions, The chemical potential of water in aqueous solutions of potassium and sodium phosphates and arsenates at 25°, J. Phys. Chem. 58 (1954) 596–602.
[61] H.F. Holmes, R.H. Busey, J.M. Simonson, R.E. Mesmer, D.G. Archer, R.H. Wood, The enthalpy of dilution of HCl(aq) to 648 K and 40 MPa thermodynamic properties, J. Chem. Thermodyn. 19 (1987) 863–890.
[62] P. Velho, L.R. Barroca, E.A. Macedo, A geometric approach for the calculation of the nonrandomness factor using computational chemistry, J. Chem. Eng. Data (2023).
[63] R.C. Phutela, K.S. Pitzer, Heat capacity and other thermodynamic properties of aqueous magnesium sulfate to 473 K, J. Phys. Chem. 90 (1986) 895–901.